Effects of High Intensity Ultrasound Frequency and High-Speed Agitation on Fat Crystallization

Journal:	*Journal of the American Oil Chemists Society*
Manuscript ID	JAOCS-17-0153.R1
Manuscript Type:	Original Article
Date Submitted by the Author:	n/a
Complete List of Authors:	Silva, Roberta Lee, Juhee Martini, Silvana; Utah State University, Department of Nutrition and Food Sciences
Keywords:	Structure - Functional Properties < Food and Feed Science / Nutrition and Health, Fat crystallization < Lipid Chemistry / Lipid Analysis, Rheology < Lipid Chemistry / Lipid Analysis, Thermal Analysis < Lipid Chemistry / Lipid Analysis, Fats and oils

Effects of High Intensity Ultrasound Frequency and High-Speed Agitation on Fat Crystallization

R.C. Silva[1], J. Lee[1], V. Gibon[2], and S. Martini[1*]

[1]Department of Nutrition, Dietetics, and Food Science, Utah State University, 8700 Old Main Hill, Logan, UT 84322-8700

[2]Desmet Ballestra R&D Center, Desmet Ballestra Group, Zaventem, Belgium

*Corresponding author: Silvana Martini, Professor, Department of Nutrition, Dietetics, and Food Sciences, Utah State University, 8700 Old Main Hill, Logan, UT, 84322-8700, silvana.martini@usu.edu, 435-797-8136

Abstract: The objective of this research was to examine the effect of ultrasound frequency and high-speed agitation on lipid crystallization. Interesterified soybean oil was crystallized at 44 ºC without and with the application of high intensity ultrasound (HIU – 20 and 40 kHz) or with high-speed agitation (6,000 and 24,000 rpm). Two tip amplitudes (24 µm and 108 µm) and three pulse durations were evaluated (5, 10, and 15 s) for the acoustic frequencies tested. Sonication at 20 kHz of frequency significantly reduced crystal size, increased ($p < 0.05$) elasticity (435.9 ± 173.3 Pa to 80,218 ± 15,384 Pa) and SFC (0.2 ± 0.0 % to 4.5 ± 0.4 %). No significant difference was observed in the crystallization behavior of these samples when sonicated at different amplitudes for 5 and 10 s. The crystallization behavior was significantly delayed ($p < 0.05$) in samples sonicated using 108 µm amplitude for 15 s. Larger crystals were formed in samples sonicated at 40 kHz compared to those obtained with 20 kHz and lower SFC (3.7 ± 0.0 %) and elasticity (3,943 ± 1,459 Pa) values were obtained. High-speed agitation at 24,000 rpm increased SFC (5.5 ± 0.1 %) and crystallized area and decreased the elasticity (42,602 ± 11,775 Pa) compared to the samples sonicated at 20 kHz.

Keywords: Interesterified oil, crystallization behavior, sonication, ultrasound, high speed agitation

Introduction

The use of power ultrasound or high intensity ultrasound (HIU) has recently been of interest to researchers in the food processing area. HIU generates safe, non-toxic, and environmentally friendly sound waves with frequencies between 20 and 100 kHz and power levels between 1 and 10,000 W cm^{-2}. Under these sonication conditions acoustic waves propagate through a medium generating high and low density zones due to partial displacement of particles. These zones of differential particle density induce cavitation [1]. Cavitation is usually referred to as the formation of a void in a liquid that grows to form bubbles. When cavitation is induced by acoustic waves, the phenomena is called acoustic cavitation. During acoustic exposure, these bubbles or cavities oscillate around their equilibrium position or they grow over time with an eventual collapse. Bubble collapse is associated with micro-currents and important increases in temperature and pressure in the media and with the generation of high shear forces [2]. The ability of ultrasound to cause cavitation depends on ultrasound process parameters such as frequency and power, intrinsic properties of the product such as viscosity and surface tension, and processing conditions such as temperature and pressure [3].

Events associated with the formation and collapse of the cavities are responsible for several physicochemical changes in materials [4] such as cell disruption, emulsification, dispersion of aggregates, crystallization, enzyme inactivation, drying, and viscosity modification among others [5-15]. In particular, HIU has been used by several research groups to change the crystallization behavior of fats [15-25]. This process is commonly referred to as sonocrystallization and the effects reported across these systems include induction in crystallization, generation of smaller and more uniform crystal sizes, induction of stable polymorphic forms, and generation of harder materials. The mechanisms

responsible for sonocrystallization in lipids have not been totally clarified. Some researchers believe that sonocrystallization occurs through an induction in nucleation since cavities or bubbles provide a heterogeneous surface for nucleation [26]. However, others argue that the effect is counterintuitive in that a local temperature increase will reduce or eliminate the supersaturation in the immediate vicinity effectively removing the driving force for nucleation. However, shock waves generated during sonication may contribute to nucleation in the regions of the supersaturated solution somewhat remote from the cavitation event [2]. In the case of lipid sonocrystallization, localized high pressures generated during sonication might result in localized increase in supercooling thus inducing crystallization. Changes observed in crystal size and morphology can be related to the shear forces associated with ultrasound that act to slow growth processes [27] and to break down nascent agglomerates [28].

Most of ultrasound studies in fat systems have evaluated the effects of ultrasound power levels and pulse duration [15, 18, 19, 25], moreover these previous studies were limited to a single frequency (20 kHz). It is still unclear if the same induction in crystallization can be generated with a higher acoustic frequency and if the effects observed during lipid sonocrystallization are due to the presence of cavities, high shear forces, or a combination of both events. Therefore, the objective of this study is to: (i) evaluate the effect of acoustic frequency on sonocrystallization and (ii) understand the role of agitation in the sonication process. With this purpose commercial interesterified soybean oil (45% saturated fat) was crystallized at 44 ºC and treated with two acoustic frequencies (20 and 40 kHz) and with high-speed agitation. The physical properties such as crystal microstructure, melting behavior, solid fat content, and elasticity, of the crystallized material obtained were measured.

Material and Methods

Material

Commercial interesterified soybean oil (IESBO) with 45% saturated fat (ADM 762420) was crystallized at 44 ºC without and with the application of high intensity ultrasound (HIU) or with high-speed agitation.

Methods

Melting Point

The melting point of IESBO (52.8 ± 0.1) was determined by DSC using a DSC Q20 (TA Instruments, New Castle, DE). The samples were heated from 25 ºC to 80 °C at 5 ºC/ min, holding at this temperature for 30 min and cooled to -20 ºC at 5 ºC/min to crystallize the sample and holding at this temperature for 90 min. After this procedure, the samples were heated again to 80 °C at 5 °C/min. Melting temperature was considered as the peak temperature of the highest temperature melting peak.

Triacylglycerol (TAG) and diacylglycerol (DAG) composition

The TAG composition of IESBO (Table 1) was analyzed by reversed phase high performance liquid chromatography (HPLC) based on the official AOCS method Ce 5b-89. Minor practical adjustments to the flow rate and mobile phase composition was made for optimal performance of the equipment. The analysis was performed on a Waters HPLC system (Zellik, Belgium) equipped with two stainless steel Nova-Pak C18 columns (4 µm, 3.9 x 150 mm) from Waters (Zellik, Belgium). The mobile phase was an isocratic solvent mixture of acetone and acetonitrile (62.5/37.5, v/v) with a flow rate of 1.2 ml/min; the

injection volume was 20 µl. The samples were dissolved in methanol/chloroform (1/1, v/v) and a differential refractometer was utilized for the detection. The partition number (PN) also called equivalent carbon number (ECN) is used to predict the elution order. PN (ECN) = CN – 2 x DB, where CN is the total carbon number and DB is the total number of double bonds on the fatty acids. Peak areas were correlated with the quantities of DAG/TAG in the oil or fat sample. The data were integrated by using the program Empower Pro with a generic Apex Track method for integration. Peak areas below 4000 area counts (equivalent to approximately 0.04% of the total peak area) were not taken into account.

Crystallization Experiments

Samples were melted in a microwave oven and then kept in an oven at 80 °C for 30 min to eliminate crystal history. The melted sample (100 g) was transferred to a double-walled crystallization cell connected to an external water bath that allowed for temperature control (44 °C). This crystallization device was previously described in Martini et al. [18]. The sample was stirred for 10 min using a magnetic stirrer (200 rpm) to improve heat transfer. The crystallization behavior of the samples was followed as a function of time for 90 min. Crystal morphology and solid fat content were monitored during crystallization using a polarized light microscope and pulsed nuclear magnetic resonance equipment (p-NMR) at 44 °C, respectively. Physical properties such as melting behavior and viscoelasticity were measured after 90 min of crystallization time at 44°C.

Ultrasound Application

HIU was applied to the samples after 45 min when a slight turbidity was observed that indicated the presence of crystals. Previous research in our laboratory has shown that greater induction in crystallization is observed when HIU is applied at the onset of crystallization

[18, 24]. A Misonix Sonicator 3000 (Misonix Inc., Farmingdale, NY, USA) operating at a frequency of 20 kHz and a custom-made Qsonica Sonicator Q500 (Qsonica, Newtown, CT, USA) operating at a frequency of 40 kHz were used to apply the ultrasound pulse. HIU was applied using a 1/2″-diameter tip operating at two tip amplitudes (24 µm and 108 µm) and at three pulse durations (5, 10, and 15 s).

Application of High-speed Agitation

Samples were crystallized as described above and high-speed agitation was applied using an Ultraturrax (IKA – Labortechnik, Staufen, Germany) at 45 min into the crystallization process. Two probes were used: (a) small probe (S18N 10g - circumference speed max: 9.8 m/s) and (b) big probe (S18N – 19g - circumference speed max: 16.6 m/s). Each probe was used at 2 speeds: (a) 6,000 rpm and (b) 24,000 rpm for 10 s.

Measurement of Solid Fat Content (SFC)

Samples were kept in the cell until the application of sonication or high-speed agitation and then transferred to p-NMR tubes and a test tube using a 10-ml pipettor. Tubes were kept in a water bath set at crystallization temperature (T_c) of 44 ºC. Tubes were tempered at T_c in the water bath before the sample was transferred. The crystallization behavior of the samples was followed by measuring SFC. SFC values of samples during crystallization at 44 ºC were measured using a NMR minispec mq 20 analyzer (Bruker, California, USA). SFC was measured as soon as the sample was taken out of the crystallization cell and every 2 min until the end of crystallization (90 min).

Crystallization Kinetics

The SFC vs. time data were fitted to the reparametrized Gompertz model (eq. 1).

$$SFC\ (t) = SFC_{max}\left(\exp\left\{-ex\left[\mu\ x\ 2.781281\ x\ \left(\frac{1-x}{z}\right)+1\right]\right\}\right) \quad [1]$$

The parameter SFC_{max} (%) is related to the final SFC, μ (%·min^{-1}) is related to the maximal growth rate, whereas λ (min) is the induction time of crystallization. This equation has been used previously to describe isothermal crystallization of fats [29-31].

Crystal Microstructure

Crystal morphology was recorded during crystallization using a polarized light microscope (PLM-Olympus BX 41 America Inc., Melville, NY, USA) with a digital camera (Lumenera Scientific, Infinity 2, Ottawa, Ontario, Canada) attached and a temperature-controlled stage (Instec, TS62, Colorado, USA) to allow for temperature control during the measurement. A 20 X magnification objective was used. PLM images were taken every 10 min throughout the crystallization experiment at 44 °C.

Melting Behavior

The melting behavior of the crystallized material was evaluated using a differential scanning calorimeter (DSC-TA Instruments, New Castle, DE, U.S.A.). The crystallized material (5−15 mg) was placed in a hermetic aluminum pan and heated from T_c (44 °C) to 80 °C at 5°C/min to evaluate its melting behavior. Melting parameters such as onset temperature (T_{on}; the temperature at which the sample starts melting), peak temperature (T_p; the temperature at which the melting peak reaches its maximum), and melting enthalpy (energy required for melting) were recorded.

Viscoelastic Properties

A magnetic bearing rheometer (TA Instruments AR-G2, New Castle, DE, USA) was used to evaluate the viscoelastic properties of the material after 90 min of crystallization. A temperature-controlled standard size recessed end concentric cylinders geometry (15.17 mm diameter - 991036) was used. The geometry temperature was set at 44 °C and a gap of 4000 μm was used for these measurements. Oscillatory tests were performed by strain sweep step to obtain viscoelastic parameters such as the storage modulus (G′) from the linear viscoelastic region.

Statistical Analysis

Crystallization experiments were performed in triplicate and physical properties were measured in triplicate (SFC and crystal microstructure) and duplicate (DSC and elasticity). Significant differences ($\alpha = 0.05$) were evaluated using two-way ANOVA using GraphPad Prism software, version 6.00 for Windows (GraphPad Software, San Diego, CA, USA).

Results and Discussion

Solid fat content

Figure 1 shows the crystallization behavior of IESBO measured by SFC as a function of time when different acoustic amplitudes and pulse duration were used at 20 kHz (Figure 1A), 40 kHz (Figure 1B), and high-speed agitation (Figure 1C). The solid fat content after 90 min of crystallization of sonicated and high-speed agitated samples are shown in Table 2.

Figure 1A shows the curves of SFC for non-sonicated IESBO and for sonicated at 20 kHz. Non-sonicated IESBO started crystallizing at 44 min and SFC did not increase in a significant manner over the 90 min of crystallization with a final SFC of 0.2%. The SFC of all sonicated samples increased over time in a sigmoidal manner, reaching a plateau

approximately after 75 min for amplitudes 24 μm and 108 μm with 10 s pulse (3.7 ± 0.2% and 3.9 ± 0.2% respectively), indicating that an equilibrium of SFC [32] was first established for these samples compared to the ones sonicated using 108 μm amplitude for 5 s that reached the plateau after 83 min of crystallization (4.3 ± 0.04%) and 108 μm amplitude for 15 min in which the plateau was reached almost at the end of the experiment at 90 min (3.7 ± 0.21%). SFC values were fitted to the Gompertz equation and all sonicated samples were well fitted with R^2 values above 0.91 (Table 3). Non-sonicated samples did not fit the Gompertz equation (R^2 = 0.71) since its SFC did not increase as a function of time and remained close to zero. IESBO sonicated with 24 and 108 μm for 10 s had shorter induction times (51.1 ± 0.7 and 50.8 ± 0.5 min) and a significant ($p < 0.0001$) greater growth rate (0.2 ± 0.0 and 0.2 ± 0.0 % min^{-1}) when were compared to the other sonication conditions at 20 kHz. Results obtained for the same amplitude (108 μm) suggest that pulse duration plays an important role to promote crystallization. The pulse time of 5 s was short and probably not enough cavitation was generated to promote nucleation resulting in a slower crystallization. On the other hand, a longer pulse duration such as 15 s produced a significant ($p < 0.001$) delay on induction time (58.0 ± 1.0 min) that may be associated with increases of temperature (ΔT = 5.6 °C) (Table 4) during the sonication. This increase in temperature is associated to the dissipation of acoustic energy converted into heat [33]. Table 4 shows the temperature increase for all sonicated samples. This table shows that the greatest temperature increase was observed for the IESBO sonicated at 20 kHz for 15 s using a 108 μm pulse. Even though sonication for longer times increased the induction time due to an increase in temperature the SFC after 90 min was similar to the other sonicated samples ($p > 0.05$, Table 2). These facts suggest that the thermal effect generated by HIU in longer pulse durations can promote undesirable effects in the crystallization kinetics.

Figure 1B shows SFC values as a function of time for the sample crystallized with and without HIU at 40 kHz frequency. As observed for 20 kHz, sonicated IESBO using 40 kHz waves presented higher values ($p < 0.0001$) of solid fat content (Table 2) than those observed in the sample crystallized without HIU (0.2 ± 0.0%) indicating that a sonication frequency of 40 kHz also induced crystallization. However, SFC values obtained with 40 kHz frequency were slightly lower than those observed at 20 kHz frequency after 90 min (Table 2) but these differences were only significant ($p < 0.0001$) for sample crystallized at 24 μm for 10 s and at 108 μm for 5 s. This suggests that sonication using 40 kHz frequency is also able to induce crystallization; however, higher power levels are needed to obtain a similar SFC after 90 min. When using 40 kHz frequency and amplitude of 108 μm for 15 s, the plateau was reached after 77 min of crystallization, whereas when the same amplitude was applied for 10 s SFC values reached a plateau after 87 min. Only samples sonicated using 108 μm amplitude for 10 and 15 s were well fitted to the Gompertz equation with R^2 values above 0.90 (Table 3). This lack of fit for the milder sonication conditions (24 μm for 10 s and 108 μm for 5 s) is explained by the slow growth in SFC where the shape of the SFC curve did not follow a sigmoidal shape (Figure 1B). The kinetics parameters show that IESBO sonicated using amplitude of 108 μm for 10 and 15 s had induction times of 51.9 ± 1.2 and 51.8 ± 0.7 min, respectively which were in the same order of magnitude than the ones obtained for the IESBO sonicated at 20 kHz. Sonication conditions at 20 kHz that had the greater effect on SFC curves were the ones performed at 24 μm and 108 μm of amplitude for 10 s. However, these conditions did not perform well for the 40 kHz sonication conditions where the best conditions were obtained for samples sonicated at 108 μm for longer time (10 and 15 s). This again supports the hypothesis that a higher power level is needed when HIU is applied at a higher frequency such as 40 kHz compared to the 20 kHz one. In addition, it is important to note that temperature increases observed for the samples sonicated using the 40 kHz wave

are lower than the ones obtained for the 20 kHz one (Table 4) and explains the efficiency of the 40 kHz sonication at 108 μm for 15 s.

Figure 1C shows SFC values as a function of time for IESBO crystallized using high-speed agitation with two different probes and two speeds (6,000 and 24,000 rpm) for 10 s. High-speed agitation was effective in promoting crystallization as shown by a significant increase ($p < 0.0001$) in SFC for agitation values of 24,000 rpm (Table 2). As expected, higher agitation rate produces changes in crystallization [34]. With the exception of the sample crystallized using the big probe at 6,000 rpm all other high-speed treated samples were well fitted to the Gompertz model (Table 3). Kinetic parameters (Table 3) showed shorter induction time (λ) ($p < 0.001$) and slightly higher growth rate (μ) for samples agitated using the bigger probe and greater speed (24,000 rpm). The SFC after 90 min of crystallization under this condition was significantly higher ($p < 0.0001$) than the one obtained for the non-sonicated sample. Samples agitated at 24,000 rpm reached a significantly higher SFC value ($p < 0.0001$, Table 2) of 5.5 ± 0.1 % compared to the ones obtained for sonicated samples.

In order to understand differences in SFC observed between sonicated and agitated samples images and videos were captured during sonication and high-speed agitation (Figure 2, supplementary material). Figure 2A and 2B show bubbles generated during sonication using the higher tip amplitude (108 μm) at 40 and 20 kHz, respectively; while Figure 2C and 2D show bubbles generated during the use of high-speed agitation using 24,000 rpm and 6,000 rpm of speed respectively. These images show that a greater amount of bubbles and agitation is generated with the 20 kHz tip compared to the 40 kHz one for the same tip amplitude suggesting that cavitation events generated at 20 kHz and 40 kHz are different. Sonication at 20 kHz produced mostly very small bubbles associated with shear and

microstreaming events. Sonication at 40 kHz produced larger bubbles that did not dissipate so easily in the media with low shear and microstreaming. This corroborates our previous hypothesis concerning the generation of fewer cavities during sonication at higher frequencies. This hypothesis is also supported by the lower increase in temperature observed for samples sonicated at 40 kHz compared to the 20 kHz samples (Table 4).

Figures 2C and 2D show IESBO treated with high-speed agitation (24,000 rpm or 6,000 rpm) and through these images it is possible to observe that agitation levels produced by the ultraturrax at the speed of 24,000 rpm was much higher than the agitation produced by sonication (20 and 40 kHz). This higher agitation levels explain the higher SFC obtained using 24,000 rpm compared to the sonicated IESBO. However, the agitation produced at the speed of 6,000 rpm resembles that observed in the sonication using the frequency of 20 kHz. The effect of high agitation on lipid crystallization has been widely described by others [22, 35-38]. Shear greatly accelerates nucleation resulting in higher crystallization rates and an increased number of smaller crystals, which typically results in increased fat crystal network strength [38]. It is known that shear provides enough energy to overcome activation energy barriers and consequently increase the rate of primary nucleation [37]. IESBO crystallized under high-speed agitation confirmed these statements (Figure 2C and 2D).

Crystal Microstructure

Polarized light microscopy (PLM) images of crystallized IESBO with and without HIU at 44 ºC are presented in Figure 3. The crystallization of IESBO without HIU started before 50 min with the crystallization of few and weak birefringent clusters. After 90 min in the crystallization cell these few irregular clusters increased in size and birefringence, but they did not form a crystalline network, which eventually reflected the low SFC (0.2 ± 0.0%)

observed in Table 2 and Figure 1. The images shown in Figure 3 support the results discussed in the SFC section where all ultrasound treatments induced crystallization. Consequently, an increase in the crystallized area is observed in the PLM images.

As previously described for the SFC data crystal microstructure show that the frequency of 20 kHz induced crystallization, mainly using amplitudes of 24 and 108 μm for 10 s leading to a crystalline network formed by small lipid crystals and confirming the results showed by the kinetics parameters. Even though slight differences were observed in the crystallization kinetics (Table 3, Figure 1) as a function of tip amplitude and duration, the PLM images obtained after 90 min did not show significant differences in terms of crystal sizes and shapes. For IESBO sonicated at 40 kHz a slight induction in crystallization was also observed at 50 min; however, the crystalline network formed after 90 min was more open with bigger crystals compared to the ones observed using 20 kHz frequency. Likewise, images of IESBO using 40 kHz are coherent to previous results with big clusters of variable sizes were observed after 90 min of crystallization. The differences described above for SFC between 20 and 40 kHz can also been seen in the PLM images. Samples sonicated using 20 kHz of frequency induced crystallization even at the lowest amplitude and slightly bigger clusters were observed in samples sonicated for 15 s. Whereas for 40 kHz of frequency the sonication only generated enough cavitation to form a crystalline lattice when the largest amplitudes were used at higher pulse times (108 μm for 10 and 15 s)

High-speed agitation induced fast crystallization mainly using 24,000 rpm independently of the probe used (Figure 4). After 50 min of crystallization, several small crystals were observed confirming the short induction time (48.8 ± 1.4 min and 44.8 ±1.1 min) reported in Table 3 compared to sonicated IESBO. After 90 min of crystallization, high-speed agitation at 24,000 rpm showed a homogeneous area of small spherulites and a

crystalline network comparable with the ones obtained with sonication at 20 kHz. The effect of agitation on crystal size was described by others [34, 39] showing perhaps evidence of a secondary nucleation caused by crystal contact mechanism [37].

High-speed agitation at 6,000 rpm also induced crystallization but after 50 min of crystallization only few big crystals were observed that after 90 min formed a dense network with heterogeneous clusters and voids between these clusters. Probably this speed (6,000 rpm) was not high enough to induce as much nucleation as the one generated using 24,000 rpm but was enough to enhance the rate of heat and mass transfer and to promote crystal growth [40].

Melting Behavior

Figure 5 shows the melting profile of IESBO measured by DSC when di□erent acoustic amplitudes and pulse duration were used at 20 kHz (Figure 5A) and 40 kHz (Figure 5B) frequencies and high-speed agitation (Figure 5C). Table 5 shows onset (T_{on}, °C), peak temperatures (T_p, °C), and melting enthalpy (ΔH, J/g) obtained from these melting thermograms (Figure 5).

DSC thermograms of the non-sonicated IESBO and of the IESBO sonicated with 20 kHz frequency (Figure 5A) show that sonication produces changes in the melting profiles. The melting profile of the non-sonicated IESBO showed a main peak at 51.7 ± 1.2 °C with a shoulder at 59.39 ± 1.25 °C indicating some level of fractionation. IESBO sonicated at a frequency of 20 kHz using 24 µm of amplitude for 10 s and 108 µm of amplitude for 5 and 10 s showed melting profiles with only one peak, and this peak was sharper than the one obtained for the non-sonicated sample and no shoulder was observed at higher temperatures. This sharper melting peak suggest co-crystallization of the triacylglycerols (TAGs) promoted

by sonication. Although no significant differences ($p > 0.05$) were observed in T_p of sonicated and non-sonicated samples (Table 5) values obtained for sonicated samples were slightly lower that the ones obtained for the non-sonicated ones. The enthalpy of samples sonicates using 24 μm amplitude for 10 s and 108 μm amplitude for 5 and 10 s were significantly higher ($p < 0.05$) than the ones obtained for the non-sonicated samples (Table 5) indicating that the amount of crystallized fat was significantly higher for these samples, which correspond to the higher SFC obtained after 90 min of crystallization (Table 2). However, for samples sonicated using 108 μm amplitude for 15 s the melting profile showed a wider peak similar to the one observed for the non-sonicated IESBO. In addition, even though enthalpy values for this sonicated sample was higher than the one obtained for the non-sonicated sample, this difference was not significant ($p > 0.05$).

Sonication at 40 kHz did not affect melting profiles in a significant manner as melting peaks of all sonicated samples were broad as the ones observed for the non-sonicated samples (Figure 5B). Moreover, no differences ($p > 0.05$) were observed in T_p or in melting enthalpy values among the sonicated and non-sonicated samples. This lack of effect on the melting behavior is probably due to the low degree of cavitation obtained at this frequency as previously discussed.

The thermograms obtained for samples treated with high-speed agitation show that the effects in melting behavior were totally different from sonicated samples. High-speed agitation mainly at higher speeds (24,000 rpm) shows signficant fractionation as evidenced by a marked shoulder obtained at high temperatures (55.74 ± 0.39 °C). This unexpected result could be a consequence of air incoporation during high-speed agitation. The air incorporated during the agitation is cooler than the crystallization temperature and therefore induces the crystallization of high melting point TAGs. The amount of crystals was increased

as shown by the enthalpy values and this increase was only significant ($p < 0.05$) for samples crystallized using the big probe at high speed (24,000 rpm). The enthalpy values for agitation using the 24,000 rpm were related to the results observed in SFC and PLM where higher final SFC and higher crystallized area were obtained compared to the other speed.

Viscoelastic Properties

Figure 6 shows the storage or elastic modulus (G') of IESBO crystallized without and with sonication at 20 and 40 kHz (Figure 6A) and high-speed agitation (Figure 6B) crystallized for 90 min. IESBO sonicated at 20 kHz using amplitudes of 24 and 108 µm for 10 s and 108 µm for 5 s showed a significantly higher G′ ($p < 0.0001$) than the ones obtained for non-sonicated IESBO and for IESBO sonicated using 108 µm amplitude for 15 s (Figure 6A). The elasticity of sonicated IESBO at amplitudes of 24 and 108 µm for 10 s and 108 µm for 5 s at 20 kHz frequency showed the highest increments (80,218 ± 15,384 Pa, 72,735 ± 9,547 Pa and 67,727 ± 16,797 Pa, respectively) in G' compared to the non-sonicated samples (436 ± 173 Pa). The amplitude of 108 µm for 15 s was not significantly different from the non-sonicated IESBO ($p > 0.05$) probably due to the increment of 5.6 °C in temperature (Table 3) that occurred with higher pulse durations. Although there has been an increase in the elasticity of IESBO sonicated at 40 kHz these increments were not significantly different from the non-sonicated samples ($p > 0.05$) (Figure 6A).

The elasticity of the IESBO subjected to high-speed agitation (Figure 6B) was significantly higher ($p < 0.0001$) than non-sonicated ones only for samples crystallized using 24,000 rpm agitation with both probes. Despite the samples subjected to high-speed agitation showed significantly higher SFC (Table 2) and the PLM (Figure 4) showed a microstructure with a large crystallized area, which resembles the 20 kHz frequency, the G 'values for

samples crystallized under 24,000 rpm agitation were significantly ($p < 0.05$) smaller (42,602 ± 11.177 and 39,950 ± 23,828 Pa) than the ones observed for IESBO sonicated at 20 kHz (80,218 ± 15,384 Pa for 24 μm for 10 s).

These differences in elasticity of IESBO caused by the treatments (20 kHz, 40 kHz and high-speed agitation) used in this study could be attributed to differences in microstructure observed in Figures 3 and 4. Smaller crystals observed in IESBO sonicated with 20 kHz (24 μm for 10 s, 108 μm for 5 and 10 s) and high-speed agitation (24,000 rpm) are associated with higher G' values. On the other hand, the highest SFC observed in IESBO crystallized with high-speed agitation (5.5 ±0.1%) was not high enough to result in a higher elastic modulus (G'). This means that in this case crystal morphology had a greater contribution in G' value than SFC values. A similar behavior was observed by Rincón-Cardona et al. [25] when they studied the crystallization of sonicated sample of a stearic fraction of high stearic high oleic sunflower oil where a higher SFC was not correlated to higher values of G'. These authors associated this behavior to different crystal morphologies and/or polymorphic forms obtained in the systems. The elasticity depends not only of macrostructural properties of the crystalline network but it is also related to interactions that occur at the molecular level [41].

Conclusion

This research demonstrated that the HIU can induce changes in physical properties of IESBO using 20 and 40 kHz of frequency. These changes included solid fat content, microstructure, rheological and melting properties, however, these changes were more significant when using 20 kHz of frequency in specific conditions of amplitude (24 and 108 μm) and pulse time (5 and 10 s). An increase in a pulse time to 15 s for waves operating at 20 kHz showed negative effects on physical properties due to a significant increase in temperature. Even

though crystallization was also induced when higher frequencies of 40 kHz were used higher amplitude (108 μm) for long pulse duration (15 s) were needed to effectively change the physical properties since higher frequencies generated fewer cavities during sonication. High-speed agitation showed that agitation also improved the physical properties of IESBO. However samples crystallized under high speed agitation had different the melting profiles, microstructure, and the elasticity than the sonicated samples. These results suggest that the induction on crystallization by sonication is not only caused by the agitation of the system but also by cavitation events that are enhanced at lower frequencies. Results from this study help understand the unlying mechanisms that drive lipid sonocrystallization and are fundamental for the implementation of this technology in an industrial setting.

Acknowledgments: This project was supported and approved by the Utah Agricultural Experiment Station as project number 8968. Authors would like to thank Tom Tiffany from ADM for providing the samples.

References

[1] Rastogi NK (2011) Opportunities and challenges in application of ultrasound in food processing. Crit Rev Food Sci 51:705–722

[2] Bermúdez-Aguirre D, Barbosa-Cánovas G (2011) Power Ultrasound to process dairy products. In: Feng H, Barbosa-Cánovas G, Weiss J (eds) Ultrasound technologies for food and bioprocessing, Springer, New York, 445-466

[3] Dolatowski, ZJ, Stadnik, J, Stasiak, D (2007) Applications of ultrasound in food technology. Acta Sci Pol Technol Aliment 6:89-99

[4] Martini S. (2013) Sonocrystallization of Fats (SpringerBriefs in Food, Health, and Nutrition). New York: Springer

[5] Lida Y, Tuziuti T, Yasui K, Towata A, Kozuka T (2008) Control of viscosity in starch and polysaccharide solutions with ultrasound after gelatinization. Innov Food Sci Emerg Technol 9:140–146

[6] Leong TSH, Wooster, TJ, Kentish SE, Ashokkumar M (2009) Minimising oil droplet size using ultrasonic emulsification. Ultrason Sonoch 16:721-727

[7] Caia M, Wanga S, Zheng Y, Lianga H (2009) Effects of ultrasound on ultrafiltration of Radix astragalus extract and cleaning of fouled membrane, Separ Purific Technol 68:351–356.

[8] Champadrala J, Oliver C, Kentish, S, Ashokkumar M (2012). Ultrasonics Muthupandian Ultrason Sonoch 19:975–983

[9] Shanmugama A, Ashokkumar, M, (2014) Functional properties of ultrasonically generated flaxseed oil-dairy emulsions Ultrason Sonoch 21:1649–1657

[10] Abid M, Jabbar, S, Wu T, Hashim, MM, Hu B, Lei S, Zeng X (2014). Sonication enhances polyphenolic compounds, sugars, carotenoids and mineral elements of apple juice. Ultrason Sonoch 21:93-97

[11] Rossi D, Jamshidi R, Saffari N, Kuhn S, Gavriilidis A, Mazzei L (2015) Continuous-Flow sonocrystallization in droplet-based microfluidics. Cryst Growth Des 15:5519−5529

[12] Fijlkowska A, Nowacka M, Winktor A, Sleddz M, Witrowa-Rajchertfd FD (2016) Ultrasound as a pretreatment method to improve drying kinetics and sensory proprieties of dried apple. J Food Proc Eng 39:256-265

[13] Eldalatony MM, Kabra AN, Hwang JH, Govindwar SP, Kim KJ, Kim, H, Jeon BH (2016) Pretreatment of microalgal biomass for enhanced recovery/extraction of reducing sugars and proteins Bioprocess Biosyst Eng 39:95–103

[14] Jamshidi R, Rossi D, Saffari N, Gavriilidis A, Mazzei L (2016) Investigation of the effect of ultrasound parameters on continuous sonocrystallization in a millifluidic device. Cryst Growth Des 16: 4607−4619

[15] Maruyama JM, Wagh A, Gioielli LA, Silva RC, Martini S (2016) Effects of high intensity ultrasound and emulsifiers on crystallization behavior of coconut oil and palm olein. Food Res 86:54-63

[16] Higaki K, Ueno S, Koyano T, Sato K. (2001). Effects of ultrasonic irradiation on crystallization behavior of tripalmitoylglycerol and cocoa butter. J Am Oil Chem Soc 78:513–518

[17] Higaki K, Sasakura Y, Koyno T, Hachiya I, Sato K (2003) Physical analyses of gel□like behavior of binary mixtures of high□melting and low□melting fats. J Am Oil Chem 80:263–270

[18] Martini S, Herrera ML. 2008. Physical properties of low-trans shortenings as affected by emulsifiers and storage conditions. Eur J Lipid Sci Technol 110:172–182

[19] Martini S, Tejeda-Pichardo R, Ye Y, Padilla SG, Shen FK, Doyle T. (2012). Bubble and crystal formation in lipid systems during high-intensity insonation. J Am Oil Chem Soc 89:1921–1928

[20] Chen F, Zhang H, Sun X, Wang X, Xu X. (2013). Effects of ultrasonic parameters on the crystallization behavior of palm oil. J Am Oil Chem Soc 90:941–949

[21] Frydenberg RP, Hammershoj M, Andersen U, Wiking L. (2013). Ultrasonication affects crystallization mechanisms and kinetics of anhydrous milk fat. Cryst Growth Des 13:5375–5382

[22] Sato K, Bayés-García L, Calvet T, Cuevas-Diarte MÀ, Ueno S (2013) External factors affecting polymorphic crystallization of lipids. Eur J Lipid Sci Technol, 115:1224–1238

[23] Suzuki A, Lee J, Padilla S, Martini S (2010) Altering functional properties of fats using power ultrasound. J Food Sci 75:E208–E214

[24] Ye Y, Martini S. (2015). Application of high intensity ultrasound to palm oil in a continuous system. J. Agric.Food Chem. 63:319–27

[25] Rincon-Cardona JA, Agudelo-Laverde LM, Martini S, Candal RJ, Herrera ML. (2015). In situ synchrotron radiation X-ray scattering study on the effect of a stearic sucrose ester on polymorphic behavior of a new sunflower oil variety. Food Res Int 64:9–17

[26] Wohlgemuth K, Kordylla A, Ruether F, Schembecker G (2009) Experimental study of the effect of bubbles on nucleation during batch cooling crystallization. Chem Eng Sci 64:4155-4163

[27] Nalajala VS, Moholkar VS. (2011) Investigations in the physical mechanism of sonocrystallization. Ultrason Sonochem 18:345–355.

[28] Ratsimba B, Biscans B, Delmas H, Jenck J. (1999) Sonocrystallization: the end of empiricism? A review on the fundamental investigations and the industrial developments. KONA 17:38–48

[29] Kloek W, Walstra P, van Vliet T (2000) Crystallization kinetics of fully hydrogenated palm oil in sunflower oil mixtures. J Am Oil Chem Soc 77:389–398

[30] Foubert I, Dewettinck K, Vanrolleghem PA (2003) Modelling of the crystallization kinetics of fats. Trends Food Sci Technol 14:79–92

[31] Farmani J (2015) Modeling of solid fat content of chemically interesterified fully hydrogenated soybean oil and canola oil blends as a function of temperature and saturated fatty acids. Food Meas 9:281–289

[32] Toro-Vazquez, Herrera-Coronado, Dibildox-Alvarado, Charo-Alonso, & Gomez-Aldapa (2002) The avrami index and the fractal dimension in vegetable oil crystallization J Am Oil Chem Soc 79:855–866.

[33] Kentish S, Ashokkumar M (2011) The Physical and Chemical Effects of Ultrasound In: Feng H, Barbosa-Cánovas G, Weiss J (eds) Ultrasound technologies for food and bioprocessing, Springer, New York, 1-12

[34] Herrera ML, Hartel RW (2000) Effect of processing conditions on crystallization kinetics of a milk fat model system. J Am Oil Chem Soc 77:1177–1188

[35] Bayés-García L, Patel AR, Dewettinck K, Rousseau D, Sato K, Ueno S (2015) Lipid crystallization kinetics — roles of external factors influencing functionality of end products Cur Opin Food Sci 4:32–38

[36] De Graef V., Van Puyvelde P., Goderis B. and Dewettinck K. (2009). Influence of shear flow on polymorphic behavior and microstructural development during palm oil crystallization. Eur. J. Lipid Sci. Technol., 111, 290-302.

[37] Hartel RW (2001) Nucleation crystallization in foods. Aspen Publishers Inc, Gaithersburg, 145–191

[38] Tran T, Rousseau, D. (2016) Influence of shear on fat crystallization. Food Res Intern 81:157 163

[39] Martini S, Herrera ML, Hartel RW (2002) Effect of processing conditions on microstructure of milk fat fraction/sunflower oil blends. J Am Oil Chem Soc 79:1063–1068

[40] Campos R, Marangoni AG: (2014) Crystallization dynamics of shear worked cocoa butter. Cryst Growth Des, 14:1199-1210

[41] Narine S, Marangoni A (2001) Elastic modulus as an indicator of macroscopic hardness of fat crystal networks Lebensm-Wiss Technol. 34:33-40

Figure legends

Figure 1. SFC of IESBO during 90 min of crystallization at 44 °C (control, open circles). Samples were crystallized with HIU (solid symbols) operating at 20 kHz (A), 40 kHz (B) and with high speed agitation (C).

Figure 2. Images of IESBO crystallized at 44 ºC using HIU at 20 and 40 kHz and high-speed agitation.

Figure 3. Polarized-light microscopy (PLM) images of IESBO crystallized at 44 °C without and with high-intensity ultrasound pulse using 20 and 40 kHz frequency. White bar in the first picture represents 100 μm.

Figure 4. Polarized-light microscopy (PLM) images of IESBO crystallized at 44 °C without and with high-speed agitation at 6,000 and 24,000 rpm. White bar in the first picture represents 100 μm.

Figure 5. DSC melting profiles of IESBO crystallized for 90 min without and with HIU using 20 kHz (Figure 5A) and 40 kHz (Figure 5B) of frequency. Melting profiles of samples crystallized using high-speed Agitation are shown in Figure 5C.

Figure 6. Elastic modulus (G') of IESBO crystallized for 90 min without and with HIU using 20 and 40 kHz frequency (Figure 6A) and high-speed agitation (Figure 6B). Data with different letters are statistically different ($\alpha = 0.05$).

Table 1. Triacylglycerol and diacylglycerol composition (%) of IESBO.

	IESBO
DAG	0.8 ± 0.0
LLnLn	0.8 ± 0.0
LLLn	3.1 ± 0.1
LnLnO	0.2 ± 0.0
LLL	6.2 ± 0.0
OLLn	1.8 ± 0.1
PLLn	2.1 ± 0.0
LLO+OOLn	6.9 ± 0.1
PLL+POLn	10.2 ± 0.1
SLLn	0.3 ± 0.1
OOL	2.7 ± 0.1
POL+SLL+SOLn	16.7 ± 0.1
PPL+PSLn	2.6 ± 0.1
MPP	0.1 ± 0.0
OOO	0.4 ± 0.0
POO+SOL	9.8 ± 0.1
POP+PLS+SLnS	9.3 ± 0.1
GOO	0.2 ± 0.0
SOO	1.8 ± 0.1
POS+SLS	11.9 ± 0.1
PPS	0.9 ± 0.0
AOO	0.1 ± 0.1
SOS	4.0 ± 0.1
PSS	3.3 ± 0.2
BOO	0.1 ± 0.0
SSG+SAO	0.3 ± 0.1
SSS	2.9 ± 0.5

DAG: Diacylglycerols, L: linoleic acid, Ln: linolenic acid, O: oleic acid, P: palmitic acid, S: stearic acid, M: myristic acid; A: arachidic acid, G: gondoic acid; B: behenic acid

Table 2. Solid fat content of IESBO after sonication using 20 and 40 kHz of frequency and using high-speed agitation (Mean ± SD). Data with different superscripts are statistically different (α=0.05).

	20 kHz	40 kHz
Wo HIU	0.238 ± 0.028^{f}	
24 µm for 10 s	3.68 ± 0.17^{bc}	2.14 ± 0.03^{e}
108 µm for 5 s	4.29 ± 0.04^{b}	3.38 ±0.21^{cd}
108 µm for 10 s	3.95 ± 0.13^{bc}	3.42 ±0.28^{cd}
108 µm for 15 s	3.71 ± 0.21^{bc}	3.69 ± 0.02^{bc}
	High-speed agitation	
Small Probe (6,000 rpm)	3.44±0.39^{cd}	
Small Probe (24,000 rpm)	5.47±0.06^{a}	
Big Probe (6,000 rpm)	2.92±0.62^{d}	
Big Probe (24,000 rpm)	5.42±0.22^{a}	

Table 3. Kinetic parameters obtained from the Gompertz model corresponding to isothermal crystallization of IESBO without and with sonication at 20 and 40 kHz and using high-speed agitation (Mean ± SD). Data with different superscripts are statistically different (α=0.05).

		20 kHz			
	Wo HIU*	**24 µm/10 s**	**108 µm/5 s**	**108 µm/10 s**	**108 µm/15 s**
SFC$_{max}$ (%)	0.2±0.0	3.8±0.1^{c,d}	4.8±0.4^{b,c}	4.0±0.0^{c,d}	4.6±0.5^{b,c,d}
µ (% min^{-1})	0.01±0.0	0.20±0.0^{a}	0.16±0.0^{b}	0.20±0.0^{a}	0.12±0.01^{c,d}
λ (min)	46.5±3.9	51.1±0.7^{bc}	52.7±1.4^{b}	50.8±0.5^{bc}	58.0±1.0^{a}
r^2	*0.71*	*0.96*	*0.91*	*0.98*	*0.93*
		40 kHz			
	Wo HIU*	**24 µm/10 s***	**108 µm/5 s***	**108 µm/10 s**	**108 µm/15 s**
SFC$_{max}$ (%)	0.2±0.0	8.8±7.7	7.5±3.3	3.4±0.2^{d}	3.7±0.1^{c,d}
µ (% min^{-1})	0.01±0.0	0.08±0.0	0.11±0.0	0.11±0.0^{d}	0.16±0.0^{b}
λ (min)	46.2±3.9	65.1±12.8	59.9±3.7	51.9 ± 1.2^{bc}	51.8±0.7^{bc}
r^2	*0.71*	*0.85*	*0.86*	*0.92*	*0.96*
		High-Speed Agitation			
	Wo HIU*	**Small probe (6,000 rpm)**	**Small probe (24,000 rpm)**	**Big probe (6,000 rpm)***	**Big probe (24,000 rpm)**
SFC$_{max}$ (%)	0.2±0.0	3.8±0.4^{c,d}	6.3±0.7^{a}	4.1±1.4	5.7±0.2^{a,b}
µ (% min^{-1})	0.01±0.0	0.10±0.01^{d}	0.15±0.01^{b,c}	0.09±0.01	0.17±0.01^{b,a}
λ (min)	46.5±3.9	53.6±1.3^{b}	48.8±1.4^{c}	56.2±2.6	44.8±1.1^{d}
r^2	*0.71*	*0.90*	*0.90*	*0.67*	*0.93*

SFC_{max} (%) = final solid fat content, µ (% min^{-1}) = maximal growth rate, λ (min) = induction time

* ANOVA was performed only for samples that fitted to the Gompertz equation with R^2 above 0.90.

Table 4. Increase in temperature ($\Delta T = T_f - T_i$) obtained after sonication using 20 and 40 kHz frequency (Mean ± SD). T_f = Final temperature, T_i = Initial temperature,

	20 kHz	**40 kHz**
24 µm for 10 s	1.6 ± 0.4	0.2 ± 0.1
108 µm for 5 s	0.7 ± 0.3	0.5 ± 0.1
108 µm for 10 s	1.0 ± 0.2	0.6 ± 0.0
108 µm for 15 s	5.6 ± 0.8	2.1 ± 0.2

Table 5. Melting parameters of IESBO crystallized at 44 °C for 90 min without and with HIU and with high-speed agitation (Mean ± SD). Samples were sonicated using 20 kHz and 40 kHz frequency. T_{on}: onset temperature, T_p: peak temperature, and ΔH: melting enthalpy. Data with different superscripts are statistically different (α=0.05)

	T_{on} (°C)	T_p (°C)	ΔH (J/g)
		20 kHz	
Wo HIU	47.7 *	51.7 ± 1.2^{a}	6.5 ± 2.7^{d}
24 µm for 10 s	46.9 ± 1.4	49.7 ± 0.5^{a}	11.3 ± 0.6^{a,b,c}
108 µm for 5 s	46.4 ± 0.1	50.1 ± 0.5^{a}	11.7 ± 1.6^{a,b}
108 µm for 10 s	45.4 ± 0.4	49.8 ± 0.1^{a}	10.5 ± 1.1^{a,b,c}
108 µm for 15 s	46.8 ± 1.2	49.8 ± 0.9^{a}	8.5 ± 0.6^{b,c,d}
		40 kHz	
Wo HIU	47.7*	51.7 ± 1.2^{a}	6.5 ± 2.7^{d}
24 µm for 10 s	48.1 ± 0.0	51.7 ± 0.7^{a}	5.5 ± 1.7^{d}
108 µm for 5 s	46.8 ± 0.7	51.2 ± 1.6^{a}	6.5 ± 2.2^{d}
108 µm for 10 s	46.7 ± 1.0	52.6 ± 3.2^{a}	8.4 ± 0.9^{b,c,d}
108 µm for 15 s	47.8 ± 1.2	51.4 ± 2.7^{a}	7.3 ± 1.9^{c,d}
		HIGH-SPEED AGITATION	
Wo HIU	47.7*	51.7 ± 1.2^{a}	6.5 ± 2.7^{d}
Small Probe (24000 rpm)	45.9 ± 0.5	49.2 ± 0.5^{a}	10.6 ± 1.4^{a,b,c,d}
Small Probe (6000 rpm)	47.6 ± 0.4	51.0 ± 0.8^{a}	6.3 ± 1.1^{d}
Big Probe (24000 rpm)	46.2 ± 0.4	51.6 ± 2.4^{a}	12.8 ± 3.6^{a}
Big Probe (6000 rpm)	46.2 ± 0.6	49.3 ± 0.6^{a}	9.5 ± 1.6^{a,b,c,d}

*This value refers to a single measure, so the error was not established.

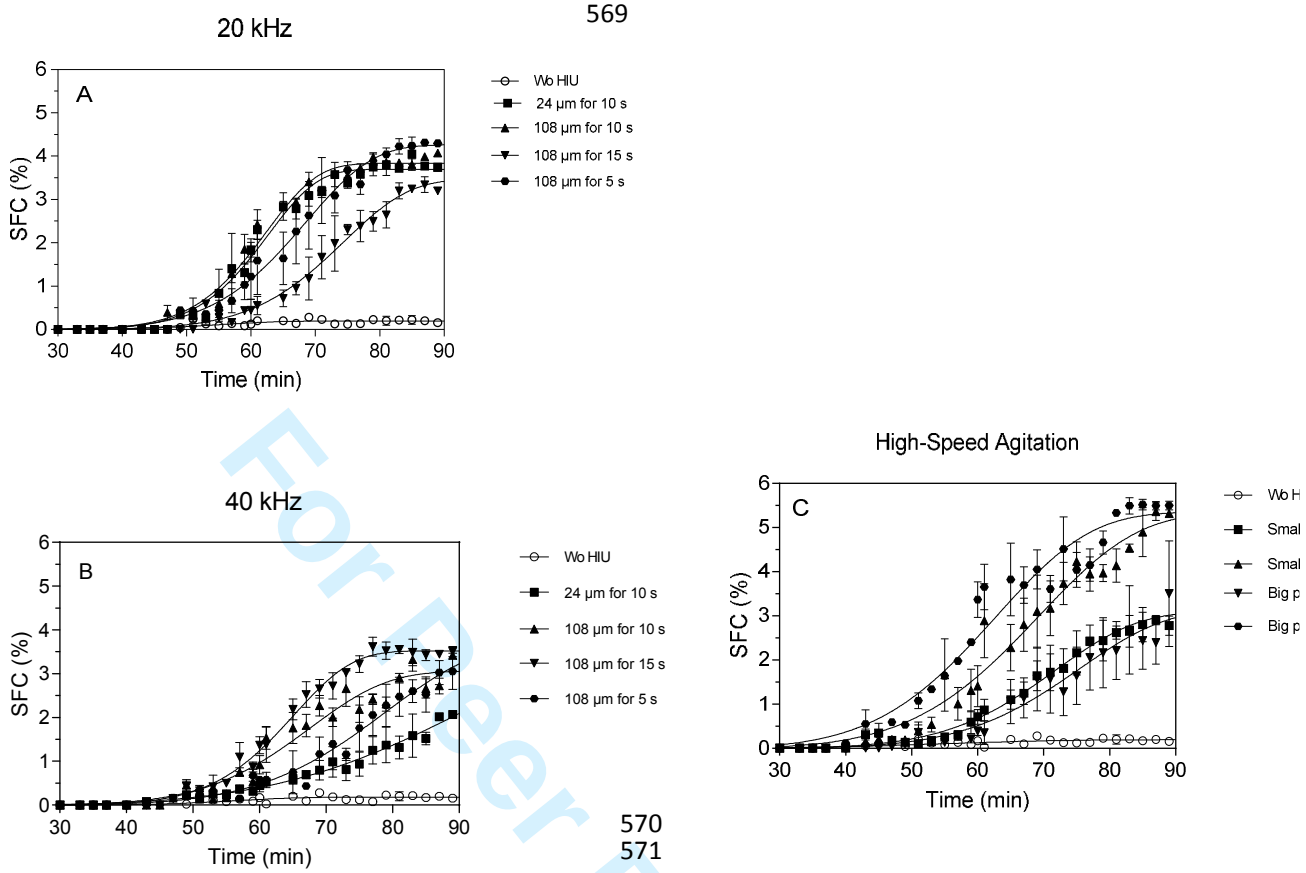

Figure 1. SFC of IESBO during 90 min of crystallization at 44 °C (control, open circles). Samples were crystallized with HIU (solid symbols) operating at 20 kHz (A), 40 kHz (B) and with high speed agitation (C).

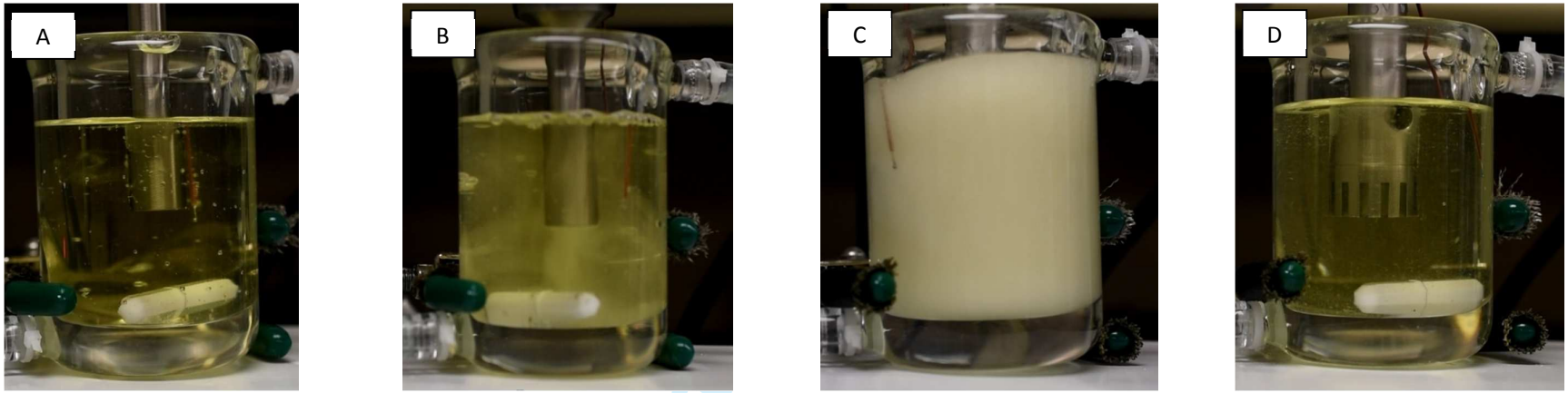

108 µm (40 kHz) 108 µm (20 kHz) High-speed agitation (24,000 rpm) High-speed agitation (6,000 rpm)

Figure 2. Images of IESBO crystallized at 44 ºC. These images were captured during the treatments of sonication at 40 kHz (A), 20 kHz (B) at amplitude 108 µm and high-speed agitation at 24,000 rpm (C) and 6,000 rpm (D) – videos are submitted as supplementary material.

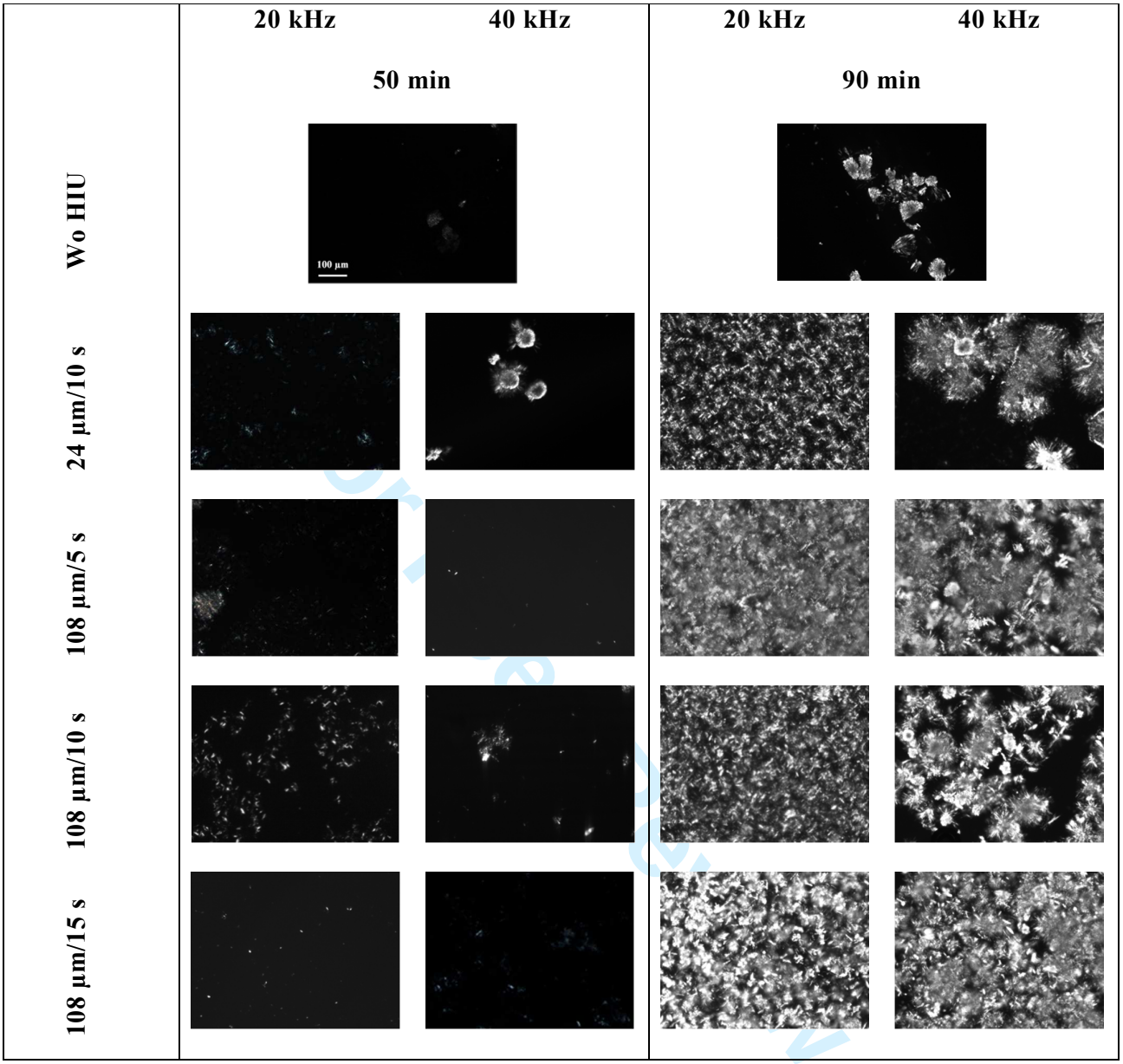

577

578 **Figure 3.** Polarized-light microscopy (PLM) images of IESBO crystallized at 44 °C without
579 and with high-intensity ultrasound pulse using 20 and 40 kHz frequency. White bar in the
580 first picture represents 100 µm.

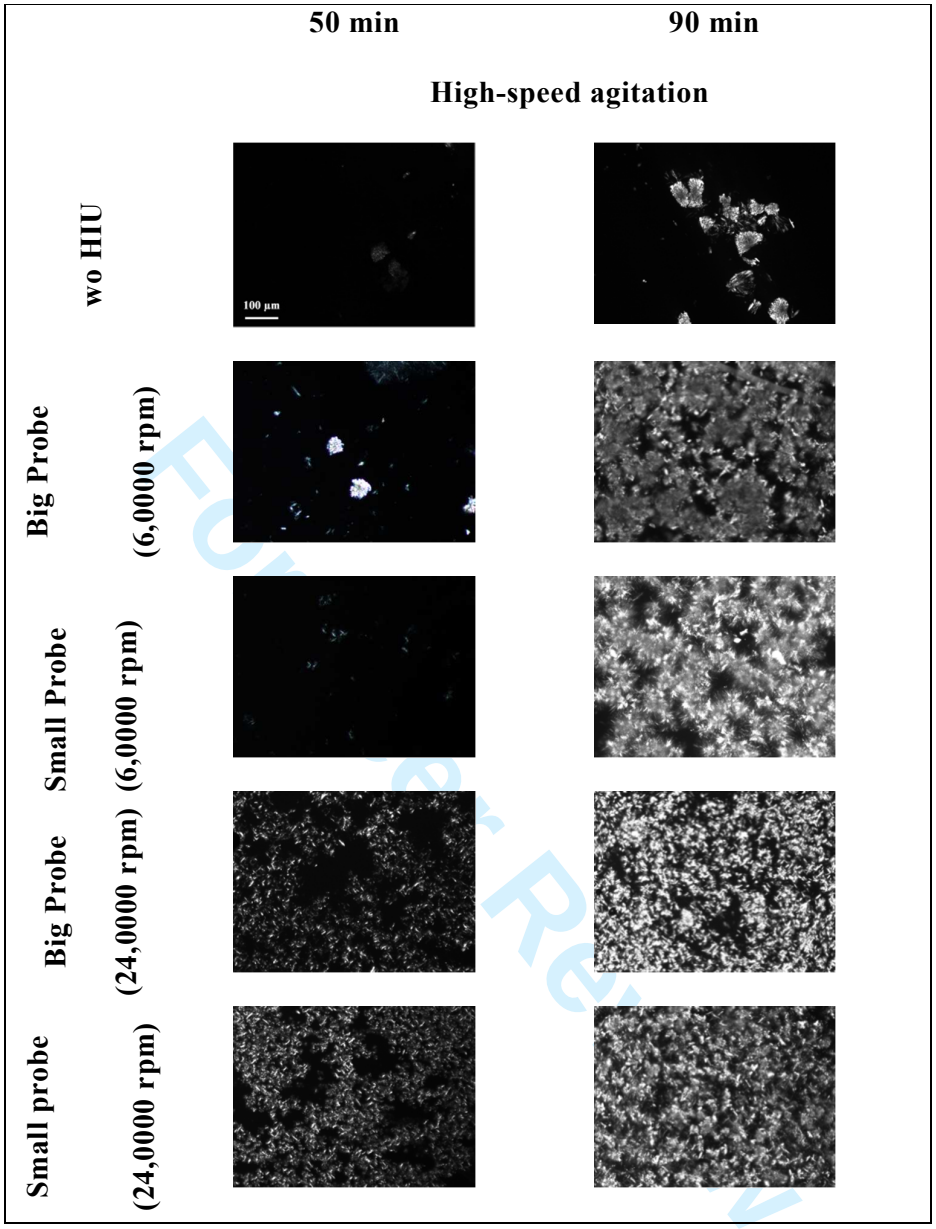

581

582 **Figure 4.** Polarized-light microscopy (PLM) images of IESBO crystallized at 44 °C without
583 and with high-speed agitation at 6,000 and 24,000 rpm. White bar in the first picture
584 represents 100 µm.

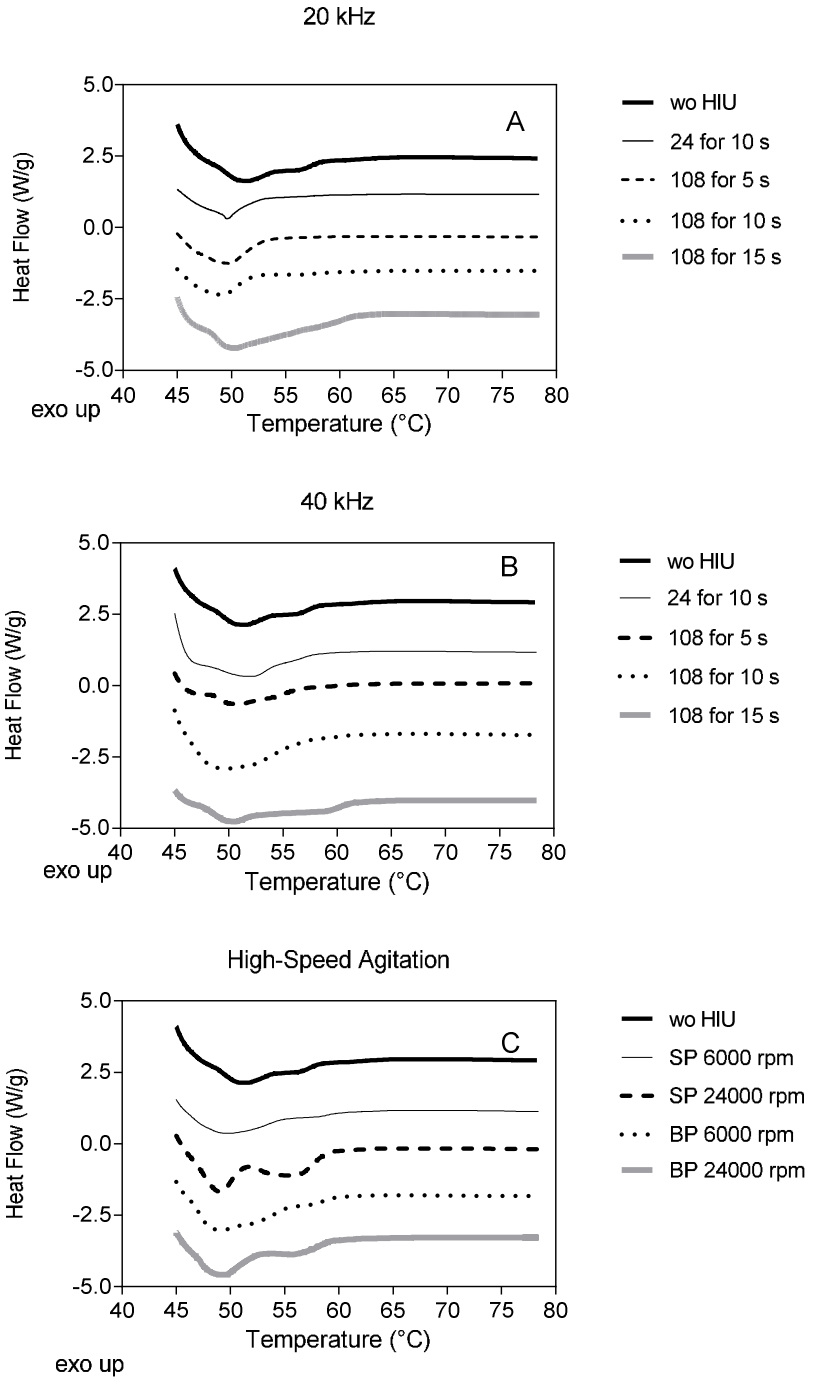

Figure 5. DSC melting profiles of IESBO crystallized for 90 min without and with HIU using 20 kHz (Figure 5A) and 40 kHz (Figure 5B) of frequency. Melting profiles of samples crystallized using high-speed Agitation are shown in Figure 5C.

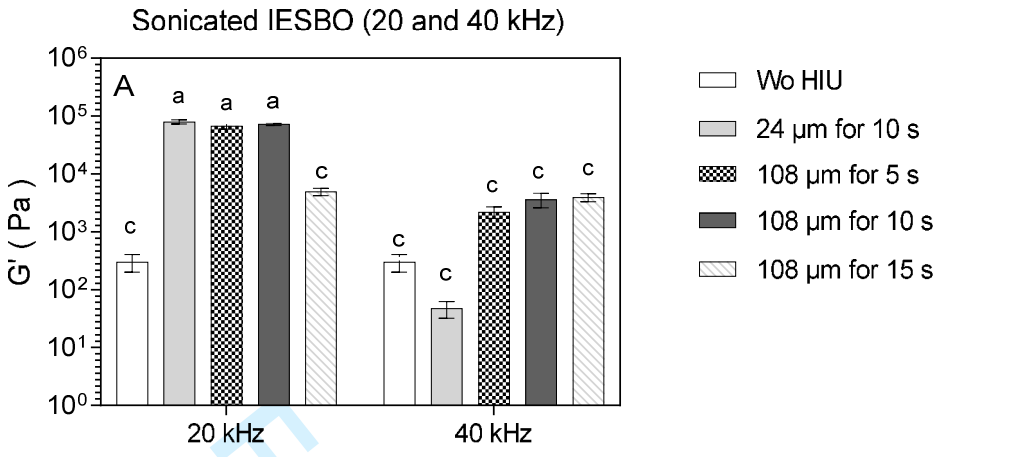

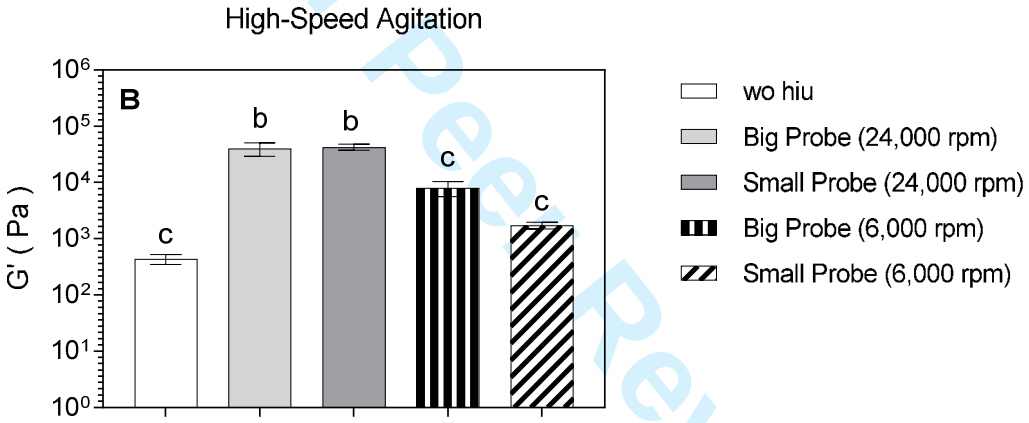

Figure 6. Elastic modulus (G') of IESBO crystallized for 90 min without and with HIU using 20 and 40 kHz frequency (Figure 6A) and high-speed agitation (Figure 6B) (Mean ± SEM). Data with different letters are statistically different ($\alpha = 0.05$)